Proceedings of the Indian National Science Academy (2026) 92:543–553
https://doi.org/10.1007/s43538-025-00433-y

RESEARCH PAPER

Accelerating photocatalytic degradation of Rhodamine B dyeby green synthesized cobalt-oxide nanoparticles using *Buteamono sperma* leaf extract

Nimisha Jadon[2] · Naorem Nanda Singh[2] · Puja Tomar[1] · Bilal Ahmad Bhat[2] · Laxmi Dubey[3]

Received: 11 September 2024 / Accepted: 4 April 2025 / Published online: 16 April 2025

Abstract

The current study aimed to synthesize green Co_3O_4 nanoparticles using leaf extract of *Butea monosperma*. Different analytical techniques like XRD, FT-IR and TEM were employed to characterize the synthesized nanoparticles. The optical properties were determined by using UV–visible spectroscopy. The green synthesized nanoparticles were further examined for the photocatalytic degradation of cationic Rhodamine B (RB) dye. Various operational parameters like irradiation time, initial dye concentration, catalyst dose, and pH affecting the degradation efficiency were evaluated and optimized. The synthesized GCo_3O_4 NPs have shown excellent photocatalytic activity (96.2%) against RB dye at optimized conditions. The study has followed Langmuir–Hinshelwood reactions kinetics with a rate constant of 0.018 min^{-1}($R^2 = 0.961$). Moreover, GCo_3O_4 has revealed good reusability for three consecutive degradation cycles. These analyses showed that GCo_3O_4 proved to be an efficient, environmentally friendly and promising material for the decomposition of dye in aqueous medium.

Keywords GCo_3O_4-NPs · *Butea monosperma* · Rhodamine B · Photocatalytic dye degradation · Kinetics

Introduction

Textile dyes and alternative industrial dyestuffs are one of the most important groups of organic compounds that are causing environmental pollution (Oller et al. 2011). Dye containing wastewater from industries pollutes the water and can alter the physicochemical properties of water, affecting the aquatic biota by reducing light penetration and affecting the rate of photosynthesis of the submerged aquatic plants (Asahi et al. 2011; Fujishima et al. 2000; Hoffmann et al. 1995). The treatment of industrial effluents containing dye has shown to be extremely difficult with conventional methods of wastewater treatment (Sun et al. 2009). The treatment of wastewater containing harmful heavy metal ions and organic dye contaminants has been successfully accomplished using techniques like adsorption and photocatalytic degradation (Cheng et al. 2014). Metal oxides are being currently utilized as efficient catalysts for the degradation of pollutants in wastewater. One of the promising and emerging materials for the effective degradation of different industrial effluents is tricobalt tetra oxide (Co_3O_4). The cobalt oxides can occur naturally and exist in a variety of oxidation states, thus makes them fascinating materials. Cobalt oxide is an amazing substance that exists in two stable phases: (i) spinel-structured Co_3O_4, which is cubic in shape and has a valence state of Co^{2+} and Co^{3+}, and (ii) cobalt oxide. Co_3O_4 exhibits p-type conductivity and is more stable than the other well-known cobalt oxide (Albargi et al. 2021). Furthermore, transition metal oxide nanoparticles with spinel structure have remarkable optical, electrical, and structural properties. The prospective uses of Co_3O_4 nanoparticles as photo-catalysts, fuel cells, energy storage, selective gas sensors, photo-thermal conversion, and random-access memory have generated a lot of interest. They are inexpensive, long-lasting, very active, and easily available. Materials based on cobalt are used as catalysts due to their significant surface active sites, electrical conductivity, and advantageous selectivity (Soni et al. 2021; Piriyadharsini et al. 2023). Biogenic

✉ Nimisha Jadon
nimisha09@yahoo.com

[1] School of Studies in Environmental Chemistry, Jiwaji University, Gwalior, M.P 474011, India

[2] School of Studies in Environmental Science (IGAEERE), Jiwaji University, Gwalior, M.P 474011, India

[3] Department of Botany, SMS, Govt. Model Science College, Gwalior, India

methods of nanoparticle synthesis often referred to as 'green synthesis' provides a viable substitute owing to non-toxicity, milder reaction conditions, and less energy utilization (Pai et al. 2022; Sodhani et al. 2022; Vinayagam et al. 2022). These methods either use plant extracts as metal ion absorbing, reducing, and capping agents, resulting in the formation of metal oxide nanoparticles (Sharma et al. 2023), or they involve the synthesis of nanoparticles using bacterial or fungal systems (Kaur et al. 2022). Few of the latest reports on cobalt oxide NPs synthesis using plant leaf extracts include *Sageretia thea* (Khalil et al. 2020), *Vitis rotundifolia* (Samuel et al. 2020), *Convolvulus arvensis* (Rasheed et al. 2018), *Helianthus annuus* (Saeed et al. 2019), and *Celosia argentea* (Shahzadi et al. 2019). However, to the best of our knowledge, no research has been published on the synthesis of cobalt oxide NPs utilizing the leaf extract of *Butea monosperma* which is native to India. Due to the presence of triterpenes, flavonoids, butein, butin, stigmasterol, í–carotene, í-sitosterol, myristic, palmitic, stearic, oleic and linolenic acids, glucoside etc., its leaf extract has wide range of potential in reducing the metals to metal oxides (Singh et al. 2015; Chaturvedi and Verma 2015).

The majority of previous studies on the use of cobalt oxide for the treatment of dyes were focused on methylene blue (MB) dye (Warang et al. 2013). In this study, Rhodamine B has been chosen as model dye pollutant. This dye is mostly utilized in textile industries, food industries as colorant, and in paper, pharmaceutical, and cosmetic sectors (Dhas et al. 2015). Intake of these dyes can cause irritation to skin, eyes and respiratory tract in human beings as well as animals (Jain et al. 2007; Amalina et al. 2022) and also results in carcinogenicity because they contain aromatic amines, which are known to cause cancer. For this reason, before releasing these dangerous substances into the environment, industries must comply with environmental regulations and remove them from contaminated industrial discharge (Srivind et al. 2020; Oladoye et al. 2022; Abdelrahman and Al-Farraj 2022). Many techniques, such as biological degradation, flocculation, electrolysis, membrane filtration, photocatalysis, adsorption, and ion exchange can be used to remove azo dyes from wastewater (Silva et al. 2016; Bhat et al. 2024a; Wan et al. 2021; Sarvalkar et al. 2023).

Among the aforementioned approaches, photocatalysis provide various benefits over other methods. One of the many advantages of photocatalysis over traditional techniques is the complete removal of contaminants and the absence of secondary pollutants (Biradar et al. 2021; Haleem et al. 2023). Due to its low cost, high retention potential, ease of use, and regeneration efficiency, photocatalysis is thought to be the most effective technology for addressing water pollution. Therefore, one of the primary goals of the current study was to synthesize GCo_3O_4-NPs utilizing extract of *Butea monosperma* leaves. Further, the green synthesized nanoparticles were used for the application of dye degradation from an aqueous medium using Rhodamine B (RB) as model dye pollutant. Various reaction parameters affecting the degradation process such as irradiation time, catalyst dose, initial dye concentration and pH were also investigated.

Experimental

Reagents & instrumentation

Rhodamine B dye was purchased from Loba Chemie Pvt. Ltd., cobaltous chloride hexahydrate, ethanol 99.9%, 0.1 M NaOH and 0.1 M HCl and all the other chemicals used were of analytical grade. Double distilled water was used throughout the study. The characterization of synthesized GCo_3O_4-NPs was performed at the Central Instrumentation Facility, Jiwaji University, Gwalior, India. Powder X-ray diffraction was done using Rigaku (Modal no Mini Flex 600) to investigate the crystallinity of the sample. Fourier transform infrared spectroscopy in the 4000–400 cm^{-1} range was employed to determine the functional groups of synthesized sample (Perkin Elmer, Modal no. Spectrum,Serial no.105627 FT-IR). Transmission electron microscopy was done using JEOL 1230 and a multipurpose UV–visible Spectrophotometer (Shimadzu UV-1280) was used to study the optical properties and photocatalytic degradation of Rhodamine B dye.

Preparation of the plant leaf extract

The fresh leaves of *Butea monosperma* were collected from the garden of the University campus (Lat: 26.20˚N and Long: 78.19˚E; Altitude: 702.5 ft). After that, the fresh leaves were washed under tap water 2–3 times and finally with double distilled water. Then leaves were spread and dried under the sunlight until they become dried so that they can be easily blended to powder by using an electric grinder. The dried leaves were blended to fine powder. After that, an amount of 10 gm of leaf powder of *B.monosperma* was added in 500 mL of distilled water and the solution was heated at 60 °C for 30 min under continuous stirring so that the biomolecules like glucoside, kino-oil containing oleic and linoleic, palmitic and lignoceric acid in the leaves are properly mixed with the water (Sharma et al. 2021). The solution was allowed to cool to room temperature and filtered. Then the filtrate (brown color) was collected and stored in a refrigerator at 4 °C and used for the synthesis of GCo_3O_4-NPs.

Synthesis of GCo_3O_4-NPs

100 mL of cobaltous chloride hexahydrate (1 M) was mixed in 100 mL of freshly prepared leaf extract with the help of a magnetic stirrer. After mixing, the solution mixture was cooled and kept overnight in a desiccator to get a dense precipitate. The precipitate was properly collected by centrifuging the solution. The precipitate was washed thrice with distilled water and absolute ethanol to remove unreacted particles and impurities. Then the precipitate was dried in an oven at 70 °C for 9 h. The dried precipitate was ground to fine powder by using a mortar and pestle. The sample was stored in glass vial for characterization and application.

Photocatalytic degradation of Rhodamine B dye

GCo_3O_4-NPs were used as photocatalyst to investigate the photocatalytic efficiency for the Rhodamine B dye. Experimental operational parameters such as effect of contact time, catalyst dose, concentration, and pH were investigated in this study. For all samples, 100 mL of aqueous dye solution was prepared and exposed to a UV lamp (6 Watt) while placed 15 cm above the solution. Before exposure to UV light illumination, the sample solution was agitated for 40 min to obtain the adsorption/desorption equilibrium. A UV–vis spectrophotometer was used to measure the absorption intensity of dye solution at regular intervals of 20 min. The color, which had been vivid, turned colorless as the dye decomposed. The following Eq. (1) has been used to calculate the percentage of dye degradation (Sarvalkar et al. 2024; Bhat et al. 2024b).

$$Degradation\,Efficiency(\%) = \frac{A_0 - A_t}{A_0} \times 100 \tag{1}$$

where, A_0 indicates the absorbance of the dye solution at time $t = 0$ min and A_t denotes the absorbance of the dye solution at the time ‘t’.

Results and discussion

Characterization

We have used Cobaltous chloride hexahydrate ($CoCl_2$ $6H_2O$) as a precursor salt to prepare the Co_3O_4-NPs. For the synthesis of GCo_3O_4-NPs, 100 mL of 1 M Cobaltous chloride hexahydrate and 100 mL of fresh leaf extract was mixed in a beaker and kept on a magnetic stirrer to form homogenous mixture. To obtain a thick precipitate, the solution combination was cooled and left in a desiccator overnight after mixing. The solution was centrifuged in order to effectively collect the precipitate. The precipitate was washed three times using distilled water and pure ethanol to eliminate impurities and unreacted particles. The resulting precipitate was dried for 9 h at 70 °C in an oven. After that, the as-synthesized cobalt oxide's structural characteristics and morphological characteristics were carefully investigated.

The XRD diffraction of the synthesized GCo_3O_4-NPs revealed that the sample is crystalline in nature (Supplementary Fig. 1a). The XRD diffraction spectrum showed prominent peaks at 2 theta 18.98°, 32.3°, 37.84°, 38.56° and 59.51° which corresponds to (111), (220), (311) (222) and (511) planes of face centered cubic (FCC) spinel crystalline phase of Co_3O_4, respectively. The peaks are well matched with the values of JCPDS card no 073–1701 (Saeed et al. 2019). The XRD results are in consistent with previous literature (Belles et al. 2021; Liu et al. 2018). The average crystallite size of the GCo_3O_4-NPs was calculated for the most intense peaks by using the Debye Scherrer’s formula (Eq. 2) and was found to be about 41.02 nm.

$$D = \frac{K\lambda}{\beta \mathrm{Cos}\theta} \tag{2}$$

where, D is the crystallite size, K is a crystallite shape factor, λ is the wavelength of X-ray, β is the full width at half maximum of the X-ray diffraction peak and θ is the Bragg’s angle.

The FTIR analysis of the synthesized material was done at the room temperature in the wave number range of 450 to 4000 cm^{-1}. A plot of the FT-IR spectra of biosynthesized Co_3O_4 NPs is shown in Supplementary Fig. 1(b1). Details on the different vibrational patterns found in the nanoparticle were provided by this spectrum. It was observed that the sample indicated prominent peaks at 3638.76 cm^{-1}, 3440.80 cm^{-1}, 2932.08 cm^{-1}, 1622.02 cm^{-1}, 1381.41 cm^{-1}, 1117.25 cm^{-1}, and 1006.04 cm^{-1} which were indicative of -OH stretching (Free), -OH stretching (H bonded), -OH broad stretching, NH_2 scissoring, -OH bending, C-O stretching (Salavati-Niasari et al. 2009; Amanullah et al. 2023) and peak at ~ 569.12 cm^{-1} was assigned to Co–O stretching vibration metal oxide bond (Karvekar et al. 2022a). The FTIR spectra of leaf extract is shown in supplementary Fig. 1(b2) and has shown bands at different wave numbers. The wide band at 3329.68 cm^{-1} can be ascribed to the hydroxyl groups (OH) of phenolic compounds and N–H stretching vibration of group NH_2. The two peaks at 2910.73 cm^{-1} and 2847.69 cm^{-1} are caused by the symmetric and asymmetric stretching of alkene molecules by -CH_2.The prominent peak that was observed at 1728.11 cm^{-1} is attributed to C = O stretching. At 1467.16 cm^{-1}, the medium peak was observed, which suggests the existence of alkane (C-H stretching). The presence of the strong peak that was observed at 1039.44 cm-1 is assigned to C–O–C stretching vibration (Rather and Sundarapandian 2022; Semwal and Kumar 2023). Biomolecules in as-synthesized GCo_3O_4 NPs exhibit a shift in peak position and peak intensity when compared to the FT-IR spectra of leaf extract due to their binding with nanoparticle surface (Pattanayak et al. 2017).

The TEM micrograph revealed that the size of the synthesized GCo_3O_4-NPs ranged from ~ 5 nm to ~ 20 nm. The TEM micrograph showed that the nanomaterial varies in shape and size showing heterogeneous distribution. Some of the particles were rounded and some were elongated in nature as shown in the Supplementary Fig. 1 (c1 &c2).

The optical characteristics of the synthesized nanoparticles were examined using UV–visible spectroscopy, which collected information between the wavelengths of 800 and 200 nm. The UV-spectroscopy analysis of the synthesized material indicated that the Co_3O_4 showed two broad absorption bands in the region 290–335 nm and 475–538 nm as shown in Supplementary Fig. 1d. These absorption bands attributed to $O^{2-} \rightarrow Co^{2+}$ and $O^{2-} \rightarrow Co^{3+}$ charge transfer transition, respectively (Abdallah and Awad 2020). The Eq. (3) was used to calculate the band gap energy of GCo_3O_4 NPs.

$$(\alpha h\nu)^2 = K\left(h\nu - E_g\right) \quad (3)$$

where, hν stands for photon energy (eV), α for absorption coefficient, K for constant, and E_g for band gap energy. The band gap can be estimated by extrapolating the linear line in the plot (Tauc plot) of photon energy (Eg) versus $(\alpha h\nu)^2$ (Amanullah et al. 2023). As can be seen from inset of Supplementary Fig. 1d, the two absorption bands give the GCo_3O_4 NPs two band gap values of 2.05 and 3.45 eV. The findings of band gap energy of GCo_3O_4 are in good agreement with previously reported studies (Dhas et al. 2015; Faisal et al. 2022).

Optimization of operational parameters for photocatalysis

Irradiation time

Dye degradation was tested at different time intervals of 20, 40, 60, 80, and 100 min for the concentration of 10 ppm of RB dye. The removal percentage was plotted against illumination time as shown in Fig. 1a and it is shown that the highest degradation for irradiation time was achieved at100 min of illumination time with 83.08% degradation. This may be explained due to the higher surface area available in the beginning for the photo-catalytic degradation. Similar studies were also reported by various researchers where an increase in irradiation time causes an increase in degradation percentage (Jadon et al. 2022; Khan et al. 2019). Considering the optimized time, the following experiments were conducted at the irradiation time of 100 min.

Dye concentration

The dye degradation was further studied at different initial dye concentrations, as it plays significant role in affecting dye degradation efficiency of the catalyst. The effect of initial dye concentration (5–40 mg/L) on photocatalytic dye degradation was examined while keeping the other parameters constant. In this study, it was found that the highest dye degradation was achieved at the concentration of 10 ppm for RB with the degradation percentage of 81.9%. The graph of the degradation percentage plotted against the variation in the concentration is shown in Fig. 1b. It was observed that with an increase in initial dye concentration to a specific limit, dye degradation efficiency also increased beyond that limit the decline in the degradation percentage was observed. Initially with an increase in dye concentration, more dye molecules were adsorbed over the catalyst surface and more active species were available to degrade dye molecules. As the concentration increase further, photocatalytic decomposition decreases due to excess dye molecules being adsorbed on the surface of photocatalyst, which inhibits photons from penetrating the catalyst surface. This result in the production of fewer electron–hole pairs and consequently lesser active radicals were generated which are the main agents responsible for the dye degradation (Dargahi et al. 2019). The results are in agreement with the previously reported literature (Sharma et al. 2021; Vishwanathan et al. 2023).

Catalyst dose

Taking the irradiation time and dye concentration at optimized conditions, the dye degradation was again examined for different catalyst doses of 10, 15, 30, 40, and 50 mg of the synthesized GCo_3O_4-NPs. The study revealed that degradation efficiency increased with increasing catalyst dose to certain limit beyond which the degradation percentage has shown a decline. The highest degradation occurs at the catalyst dose of 40 mg for the RB dye. A graph was plotted for the degradation percentage against the dosage (Fig. 1c). The results have demonstrated improvement in the dye degradation percentage from 34.2 to 87.7%. It can be concluded that increasing the quantity of catalyst increases the degradation efficiency up to a certain point, after that it decreased. A high quantity of catalyst results in a higher number of active sites on the surface, which increases the

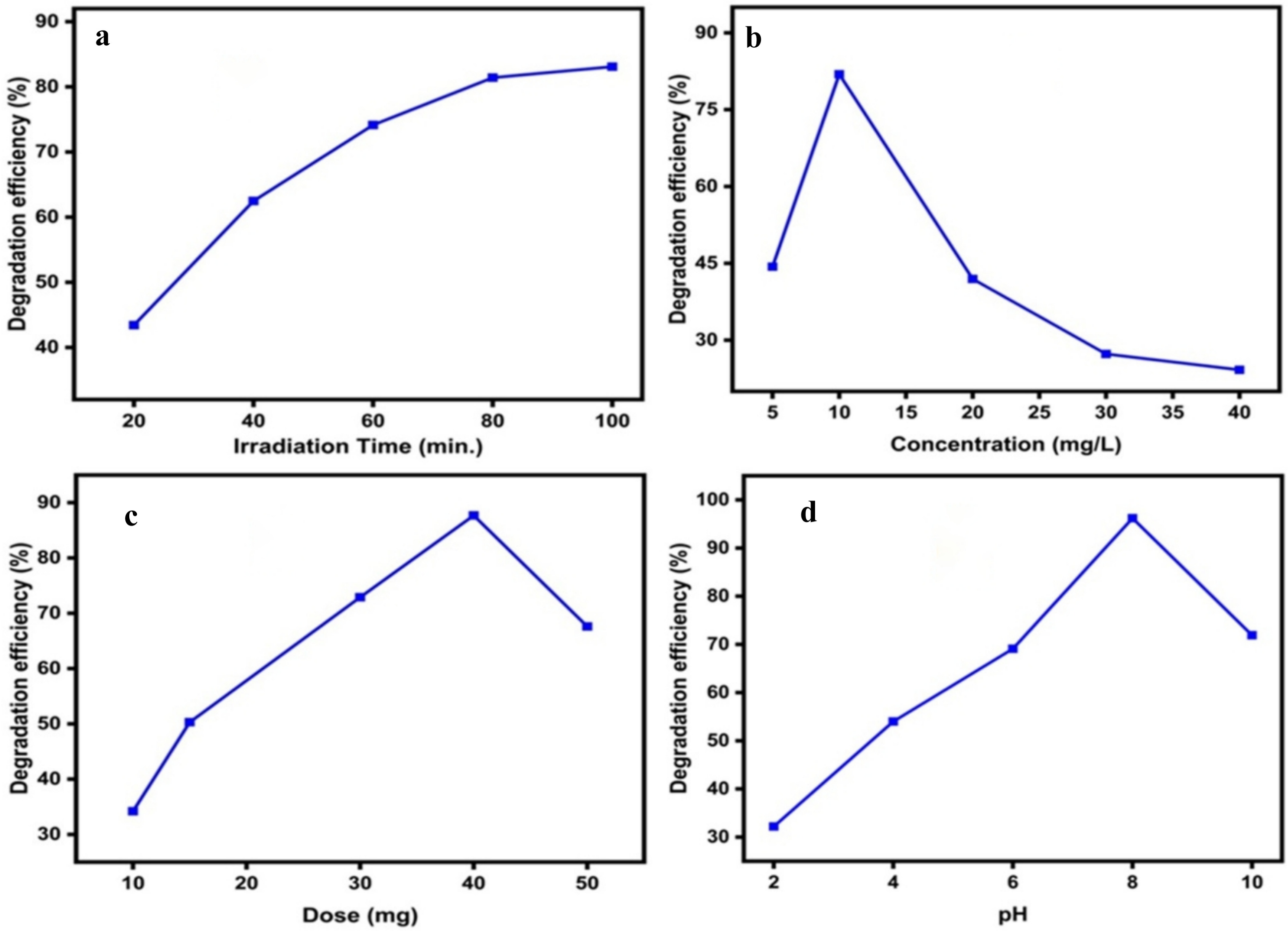

Fig. 1 **a** Effect of Irradiation time on degradation efficiency, **b** Effect of initial dye concentration, **c** Effect of catalyst dose, **d** Effect of pH on dye degradation

amount of radicals or active species that can accelerate the degradation of dye. A rise in photocatalyst quantity that surpasses a certain threshold inhibits the photocatalysis of the pollutant because it aggregates the catalyst, reducing its surface area and active sites. The turbidity of the solution, which reduces the amount of radiation that diffuses into it, is another factor causing the catalyst's effectiveness to drop (Mortazavian et al. 2019; Alshamsi et al. 2021). The previous literature has also summarized that increase in catalyst dosage to a specific quantity increases the degradation of dye from aqueous medium (Jadon et al. 2024; Priya et al. 2020; Sharma and Sharma 2021).

pH

Keeping all other parameters such as irradiation time, dose and concentration constant at their optimized values, dye degradation efficiency was studied at varying pH values (2–10). Figure 1d shows that the maximum degradation was reached at pH 8 (96.2%). The high adsorption of RB dye molecules on the catalyst surface, which result in high photocatalytic activity, may be the cause for the increase in degradation with rise of pH (Ahmad et al. 2021). Another possible explanation for this could come from the previous research work conducted by Sabour & Amiri which found that under extreme acidic conditions, H^+ ions build up on the catalyst surface. This repels the cationic RB dye molecules via electrostatic repulsion, preventing the convenient discoloration. When the pH rises to approximately 8, the concentration of H^+ ions falls, and the anionic OH^- abundance on the catalyst surface creates an electrostatic attraction with the dye that better controls the decontamination process (Sabour and Amiri 2017). Thus, RB dye being a cationic dye, promotes its adsorption on the GCo_3O_4 surface in alkaline media. Moreover, a high concentration of hydroxyl ions on the surface of GCo_3O_4 NPs in alkaline media promotes the production of hydroxyl radicals, which improves dye removal from aqueous medium. (Al-Kahtani 2016). Figure 1d illustrates the graphical plot for the degradation percentage vs. pH.

Mechanism of dye degradation

A photocatalyst forms an electron–hole pair when it absorbs photons with energy ($h\nu$) greater than or equal to the band gap energy (Eg). A hole is left in the valence band as a result of the excitation of an electron from the valence band (VB) to the conduction band (CB). The common pathway states that when Co_3O_4 was photo-excited in an aqueous solution, various radicals and charged species were formed during the photocatalytic degradation of contaminants (Viswanathan 2018; Kalaycıoğlu et al. 2023). It was possible for e^-/h^+ pairs to form inside Co_3O_4 when photons were absorbed by Co_3O_4 catalyst. The oxygen and water molecules were adsorbed on the surface of the Co_3O_4 catalyst during the photocatalytic degradation process. These molecules produce unstable hydroxyl radicals ($^{\bullet}OH$) and superoxide ions ($^{\bullet}O_2^-$) when they react with electron–hole pairs. The $^{\bullet}OH$ radical being a very strong oxidizing agent (standard redox potential of + 2.8 V on NHE) (Ribeiro et al. 2015), oxidizes the surface adsorbed organic waste into readily perishable compounds.

Thus, the Co_3O_4 NPs exhibit remarkable photocatalytic efficacy when it comes to eliminate azo dyes. The process elucidates how these NPs effectively eliminate azo dyes from aqueous solution and mineralizing them into harmless compounds like CO_2 and H_2O (Som et al. 2023; Tomar et al. 2020; Chelliah et al. 2023; Karvekar et al. 2022b). Figure 2 demonstrates the schematic illustration of RB dye degradation mechanism using synthesized nanomaterial.

Kinetics

Langmuir–Hinshelwood method was used to study the kinetics of photocatalytic degradation (Karadeniz et al. 2022). Rate constant was determined by using the pseudo first order kinetics equation as given below:

$$\mathrm{Ln}\left(A_0/A_t\right) = kt \tag{4}$$

where 'k' is the rate constant, A_0 is the initial absorbance and A_t is the absorbance of the RB dye at time 't'. The reaction rate constant and regression coefficient (R^2) given in Fig. 3b was found to be about 0.018 $min^{-1}$and 0.961, respectively. The concentration dependent curve in Fig. 3a showed the photocatalytic degradation of RB dye in presence and in absence of GCo_3O_4 catalyst.

Reuse and recycling test

The reusability of photocatalysts is crucial for their commercial application in water treatment and environmental remediation. The Co_3O_4 NPs were recovered using a centrifuge, which made it possible to separate the materials for recycling test following the photocatalysis process (Sarvalkar et al. 2023). The results, as illustrated in Fig. 4a, demonstrated that after three cycles, Co_3O_4 NPs could degrade RB dye with an efficiency of nearly 85%. The investigation concludes that green synthesized Co_3O_4 NPs are highly efficient and stable photocatalysts for dye degradation.

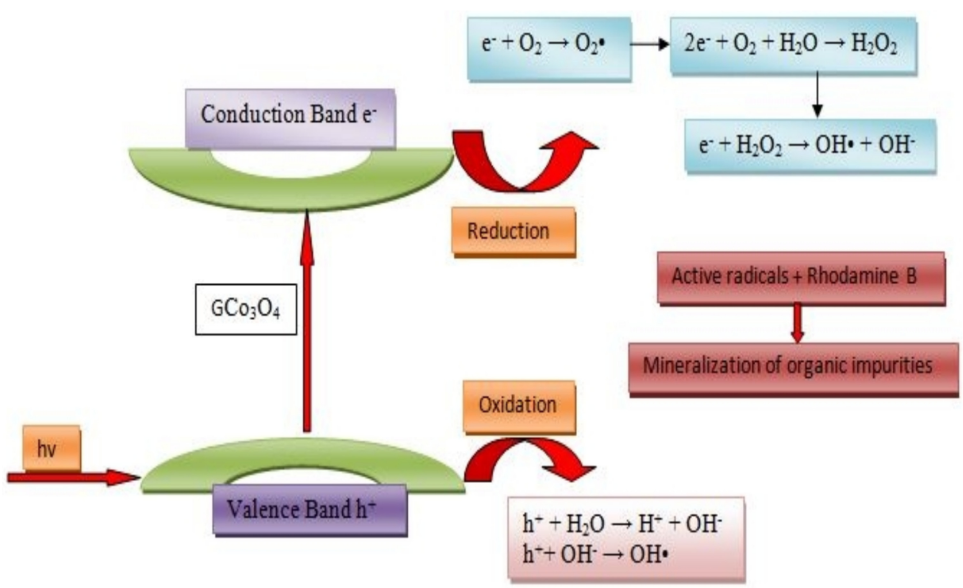

Fig. 2 Schematic diagram of photodegradation of RB

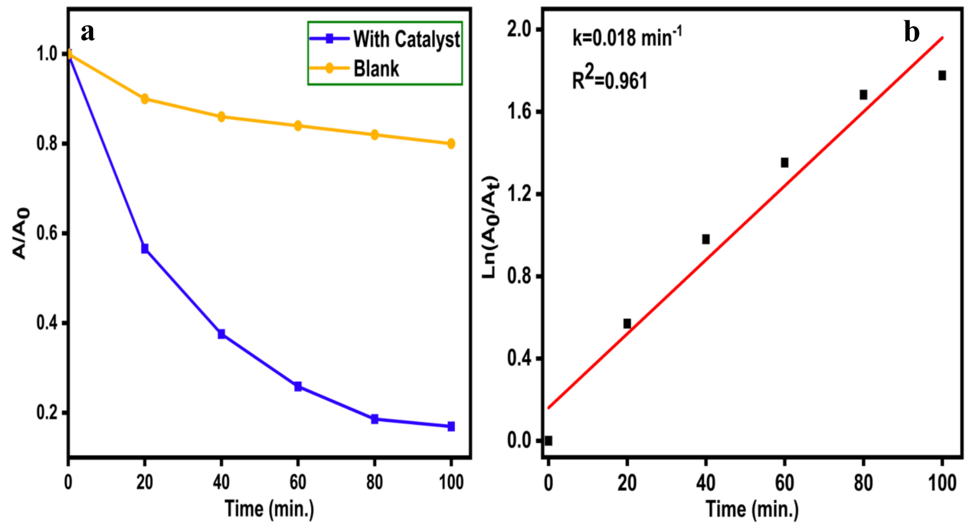

Fig. 3 **a** Degradation rate (blank) and with synthesized catalyst **b** Pseudo first order kinetic plot for photocatalytic degradation of RB

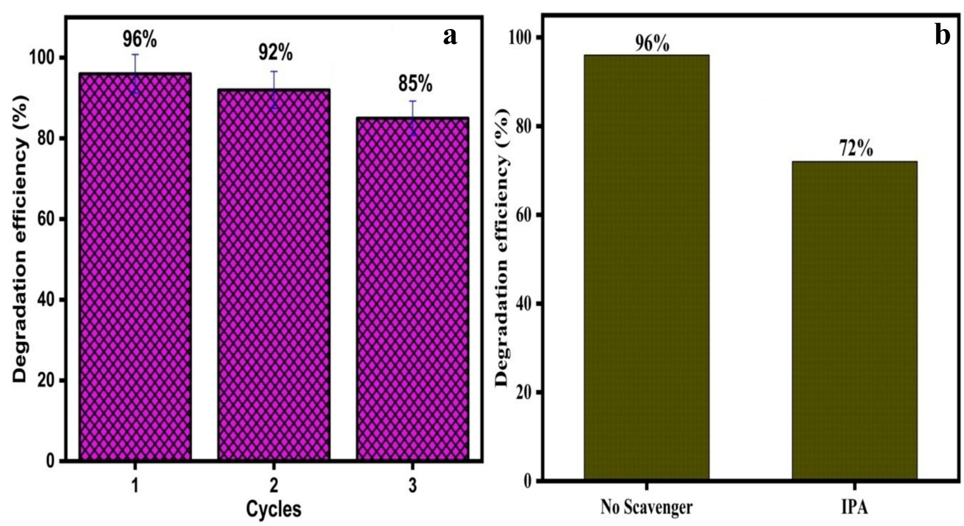

Fig. 4 **a** Degradation efficiency for three successive degradation cycles and **b** Scavenger test

Scavenger test

To establish the role of hydroxyl radicals in the degradation of dye, isopropanol (IPA) was selected as scavenger to capture the·OH radicals. Figure 4b depicts that addition of IPA caused a decrease in the photodegradation efficiency of RB dye, signifying that·OH radical play significant role in the photocatalytic process (ul Haq et al. 2024).

Comparative evaluation of the photocatalytic performance of GCo_3O_4 catalyst

The results of photocatalytic degradation of RB dye using GCo_3O_4 catalyst is compared with other metal oxide photocatalysts as mentioned in Table 1. The degradation efficiency of the synthesized GCo_3O_4 catalyst used in this work reveals a high potential for RB dye degradation.

Conclusion

To summarize, GCo_3O_4-NPs were successfully synthesized through a green route approach using leaf extract of *Butea monosperma*. The synthesized cobalt oxide NPs were characterized by XRD, FTIR and TEM analytical techniques. The X-ray diffraction characterizations revealed that the synthesized material was crystalline in nature with crystallite size < 50 nm. The green synthesized GCo_3O_4 catalyst was used for photocatalytic dye degradation. Rhodamine B dye was used as a model dye pollutant for the photocatalytic process. Various operational parameters were used to determine the degradation efficiency of the catalyst. The results of this study revealed that operational parameters have influenced the degradation efficiency of photocatalyst. The findings of this work have

Table 1 Comparison of photocatalytic performance of GCo_3O_4 catalyst with that of other photocatalysts

Photocatalyst	Dye	%Degradation	Light source	Degradation time (min.)	Ref
Ag-Co_3O_4	MO	87%	100 W incandescent light bulb	120	(Saeed et al. 2019)
Co_3O_4/g-C_3N_4	RB	97.6	Simulated sunlight	40	(Dai et al. 2023)
Mn/Ti/BC composite biochar	RB	98	UV light	90	(Yang et al. 2023)
MoS_2–TiO_2	MB	61	UV lamp	100	(Tacchini et al. 2011)
Co_3O_4	MB	93.75	400 W high-pressure mercury lamp	175	(Safdar et al. 2023)
Co_3O_4	MB	89	UVA-11 W lamp	105	(Shanmuganathan et al. 2023)
ZnO/SnO_2 composite	RB	80	UV	120	(Jansanthea et al. 2021)
GCo_3O_4	RB	96.2	UV light	100	This study

illustrated that 96.2% of RB dye was degraded at optimized conditions. The maximum degradation was achieved at an irradiation time of 100 min, with initial dye concentration of 10 mg/L, catalyst dose of 40 mg and at solution pH 8. The reaction kinetics has shown that Langmuir–Hinshelwood pseudo first-order kinetics was followed during photocatalytic process with rate constant of 0.018 min^{-1}. The recycling test has shown good reusability and better stability for three repeated degradation cycles with degradation percentage of more than 85% even after third cycle. The study reveals that GCo_3O_4-NPs synthesized by using leaf extract of *Butea monosperma* proved to be an excellent material for the degradation of RB dye and can serve as a potential material for the treatment of contaminated water. To conclude, this study provides valuable insights into the prospective application of these green synthesized GCo_3O_4-NPs for the environmental remediation.

Supplementary Information The online version contains supplementary material available at https://doi.org/10.1007/s43538-025-00433-y.

Acknowledgements The authors extend their gratitude to the Central Instrumentation Facility, Jiwaji University, India, for the assistance in the characterization of the material and School of Studies in Environmental Science for providing lab facility to conduct this study.

Funding None.

Data availability Not applicable.

Declarations

Conflict of interest The authors declare no conflict of interest, financial or otherwise.

Ethical approval Not applicable.

Research involving human and animal participants No animals/humans were used for studies that are the basis of this research.

Consent for publication Not applicable.

References

Abdallah, A.M., Awad, R.: Study of the structural and physical properties of Co_3O_4 nanoparticles synthesized by co-precipitation method. J. Supercond. Novel Magn. **33**(5), 1395–1404 (2020)

Abdelrahman, E.A., Al-Farraj, E.S.: Facile synthesis and characterizations of mixed metal oxide nanoparticles for the efficient photocatalytic degradation of rhodamine B and Congo red dyes. Nanomaterials **12**(22), 3992 (2022)

Ahmad, W., Khan, A., Ali, N., Khan, S., Uddin, S., Malik, S., Ali, N., Khan, H., Khan, H., Bilal, M.: Photocatalytic degradation of crystal violet dye under sunlight by chitosan-encapsulated ternary metal selenide microspheres. Environ. Sci. Pollut. Res. **28**, 8074–8087 (2021)

Albargi, H., Marnadu, R., Sujithkumar, G., Alkorbi, A.S., Algadi, H., Shkir, M., Sreedevi, G.: Deposition of nanostructured Sn doped Co3O4 films by a facile nebulizer spray pyrolysis method and fabrication of p-Sn doped Co3O4/n-Si junction diodes for optonanoelectronics. Sensor. Actuat. A Phys. **332**, 113067 (2021)

Al-Kahtani, A.A.: Photocatalytic degradation of rhodamine B dye in wastewater using gelatin/CuS/PVA nanocomposites under solar light irradiation. J. Biomater. Nanobiotechnol. **8**(1), 66–82 (2016)

Alshamsi, H. A., Al Bedairy, M. A., &Alwan, S. H. (2021). Visible light assisted photocatalytic degradation of Rhodamine B dye on CdSe-ZnOnanocomposite: Characterization and kinetic studies. In *IOP conference series: earth and environmental science* (Vol. 722, No. 1, p. 012005). IOP Publishing.

Amalina, F., AbdRazak, A.S., Krishnan, S., Zularisam, A.W., Nasrullah, M.: A review of eco-sustainable techniques for the removal of Rhodamine B dye utilizing biomass residue adsorbents. Phys. Chem. Earth Parts **128**, 103267 (2022)

Amanullah, A., Munir, R., Bashir, M.Z., Naz, M.Y., Shukrullah, S., Yaseen, M., Noreen, S.: Green ferrites nanoparticles synthesis using aloe vera and watermelon rinds: their applications as sorbents in the purification of direct golden yellow RL dye wastewater. Int. J. Environ. Analyt. Chem. **104**, 8778–8801 (2023)

Asahi, R., et al.: Visiblelightphotocatalysis in nitrogen-doped titanium oxides. Science **293**, 269–271 (2011). https://doi.org/10.1126/science.1061051PMID:11452117

Belles, L., Moularas, C., Smykała, S., Deligiannakis, Y.: Flame spray pyrolysis Co_3O_4/CoO as highly-efficient nanocatalyst for oxygen reduction reaction. Nanomaterials **11**(4), 925 (2021)

Bhat, B.A., Dubey, L., Sharma, M., Jadon, N.: Facile hydrothermally synthesized ZnSe/FeSe2 metal chalcogenide heterostructure composite for rapid photocatalytic degradation of organic textile dyes. Res. Chem. Int. **51**, 1–21 (2024a)

Bhat, B.A., Jadon, N., Sharma, H.K.: Exploring the photocatalytic degradation of organic textile dye using hydrothermally synthesized

Ce-doped metal chalcogenide nanomaterial. Mater. Res. Express **11**(3), 035003 (2024b)

Biradar, A.I., Sarvalkar, P.D., Teli, S.B., Pawar, C.A., Patil, P.S., Prasad, N.R.: Photocatalytic degradation of dyes using one-step synthesized silica nanoparticles. Mater. Today **43**, 2832–2838 (2021)

Chaturvedi, V., Verma, P.: Fabrication of silver nanoparticles from leaf extract of *Buteamonosperma* (flame of forest) and their inhibitory effect on bloom-forming cyanobacteria. Bioresources Bioprocessing **2**, 1–8 (2015)

Chelliah, P., Wabaidur, S.M., Sharma, H.P., Jweeg, M.J., Hasan, S., Majdi, M.M., Kubaisy, R.A., Iqbal, A., Lai, W.C.: Green synthesis and characterizations of cobalt oxide nanoparticles and their coherent photocatalytic and antibacterial investigations. Water **15**(5), 910 (2023)

Cheng, X.L., et al.: Cauliflower-like α-Fe_2O_3 microstructures: toluene–water interface assisted synthesis, characterization, and applications in wastewater treatment and visible-light photocatalysis. Chem. Eng. J. **236**, 139–148 (2014). https://doi.org/10.1016/j.cej.2013.09.089

da Silva, L.F., Barbosa, A.D., de Paula, H.M., Romualdo, L.L., Andrade, L.S.: Treatment of paint manufacturing wastewater by coagulation/electrochemical methods: proposals for disposal and/or reuse of treated water. Water Res. **101**, 467–475 (2016)

Dai, Y., Feng, Z., Zhong, K., Tian, J., Guanyu, W., Liu, Q., Wang, Z., Hua, Y., Liu, J., Hui, X., Zhu, X.: Highly efficient and exceptionally durable photooxidation properties on Co_3O_4/g-C_3N_4 surfaces. Materials **16**(10), 3879 (2023)

Dargahi, A., Samarghandi, M.R., Vaziri, Y., Ahmadidoost, G., Ghahramani, E., Shekarchi, A.A.: Kinetic study of the photocatalytic degradation of the acid blue 113 dye in aqueous solutions using zinc oxide nanoparticles immobilized on synthetic activated carbon. J. Adv. Environ. Health Res. **7**(2), 75–85 (2019)

Dhas, C.R., Venkatesh, R., Jothivenkatachalam, K., Nithya, A., Benjamin, B.S., Raj, A.M.E., Sanjeeviraja, C.: Visible light driven photocatalytic degradation of Rhodamine B and direct red using cobalt oxide nanoparticles. Ceram. Int. **41**(8), 9301–9313 (2015)

Faisal, S., Jan, F.A., Saleem, S., Ullah, R., Wajidullah, U., N., & Salman.: *J. uglansregia* L. mediated synthesis of cobalt oxide and zinc-doped cobalt oxide nanoparticles: characterization and evaluation for environmental, antibacterial and cytotoxic potential. Nanotechnol. Environ. Eng. **7**(3), 675–689 (2022)

Fujishima, A., Rao, T.N., Tryk, D.A.: Titanium dioxide photocatalysis. J. Photochem. Photobiol. Photochem. Rev. **1**, 1–21 (2000). https://doi.org/10.1016/S1389-5567(00)00002-2

Haleem, A., Shafiq, A., Chen, S.Q., Nazar, M.: A comprehensive review on adsorption, photocatalytic and chemical degradation of dyes and nitro-compounds over different kinds of porous and composite materials. Molecules **28**(3), 1081 (2023)

Hoffmann, M.R., Martin, S.T., Choi, W., Bahnemann, D.W.: Environmental applications of semiconductor photocatalysis. Chem. Rev. **1**, 69–96 (1995). https://doi.org/10.1021/cr00033a004

Jadon, N., Bhat, G.A., Sharma, M.V., Sharma, H.K.: Photocatalytic degradation of methyl orange dye with synthesized chitosan/Fe_2O_3 nanocomposite and its isotherm studies. CurrentNanoscience **18**(1), 78–85 (2022)

Jadon, N., Kour, B., Bhat, B.A., Sharma, H.K.: Green synthesis derived novel Fe_2O_3/ZnO nanocomposite for efficient photocatalytic degradation of methyl orange dye. Curr. Anal. Chem. **20**(3), 162–174 (2024)

Jain, R., Mathur, M., Sikarwar, S., Mittal, A.: Removal of the hazardous dye rhodamine B through photocatalytic and adsorption treatments. J. Environ. Manage. **85**(4), 956–964 (2007)

Jansanthea, P., Kanthabangharn, J., Chomkitichai, W., Ketwaraporn, J., Saovakon, C., Wansao, C., Wanaek, A., Kraivuttinun, P., Pookmanee, P., Phanichphant, S.: Temperature-controlled synthesis and photocatalytic properties of ZnO–SnO_2 nanocomposites. J. Aust. Ceram. Soc. **57**, 579–588 (2021)

Kalaycıoğlu, Z., ÖzuğurUysal, B., Pekcan, O., Erim, F.B.: Efficient photocatalytic degradation of methylene blue dye from aqueous solution with cerium oxide nanoparticles and graphene oxide-doped polyacrylamide. ACS Omega **8**(14), 13004–13015 (2023)

Karadeniz, D., Kahya, N., Erim, F.B.: Effective photocatalytic degradation of malachite green dye by Fe (III)-Cross-linked alginate-carboxymethyl cellulose composites. J. Photochem. Photobiol., A **428**, 113867 (2022)

Karvekar, O.S., Vadanagekar, A.S., Sarvalkar, P.D., Suryawanshi, S.S., Jadhav, S.M., Singhan, R.D., Prasad, N.R.: Bostaurus (A-2) urine assisted bioactive cobalt oxide anchored ZnO: a novel nanoscale approach. Sci. Rep. **12**(1), 15584 (2022a)

Karvekar, O.S., Sarvalkar, P.D., Vadanagekar, A.S., Singhan, R.D., Jadhav, S.M., Nimbalkar, M.S., Prasad, N.R.: Biogenic synthesis of silver anchored ZnO nanorods as nano catalyst for organic transformation reactions and dye degradation. Appl. Nanosci. **12**(7), 2207–2226 (2022b)

Kaur, T., Bala, M., Kumar, G., Vyas, A.: Biosynthesis of zinc oxide nanoparticles via endophyte*Trichodermaviride* and evaluation of their antimicrobial and antioxidant properties. Arch. Microbiol. **204**(10), 620 (2022)

Khalil, A.T., Ovais, M., Ullah, I., Ali, M., Shinwari, Z.K., Maaza, M.: Physical properties, biological applications and biocompatibility studies on biosynthesized single phase cobalt oxide (Co_3O_4) nanoparticles via *Sageretiathea* (*Osbeck*). Arab. J. Chem. **13**(1), 606–619 (2020)

Khan, A., Shah, S.J., Mehmood, K., Awais, A.N., Khan, H.: Synthesis of potent chitosan beads a suitable alternative for textile dye reduction in sunlight. J. Mater. Sci. **30**, 406–414 (2019)

Liu, J., Jin, R., Wu, Y., Wang, X., Wang, Y.: Determination of Lead (II) using glassy carbon electrode modified with hexagonal Co3O4 microparticles. Int. J. Electrochem. Sci. **13**(11), 10415–10426 (2018)

Mortazavian, S., Saber, A., James, D.E.: Optimization of photocatalytic degradation of acid blue 113 and acid red 88 textile dyes in a UV-C/TiO_2 suspension system: application of response surface methodology (RSM). Catalysts **9**(4), 360 (2019)

Oladoye, P.O., Bamigboye, M.O., Ogunbiyi, O.D., Akano, M.T.: Toxicity and decontamination strategies of Congo red dye. Groundw. Sustain. Dev. **19**, 100844 (2022)

Oller, I., Malato, S., Sanchez-Perez, J.A.: Combination of advanced oxidation processes and biological treatments for wastewater decontamination a review. Sci. Total. Environ. **20**, 4141–4166 (2011)

Pai, S., Kini, M.S., Mythili, R., Selvaraj, R.: Adsorptive removal of AB113 dye using green synthesized hydroxyapatite/magnetite nanocomposite. Environ. Res. **210**, 112951 (2022)

Pattanayak, S., Mollick, M.M.R., Maity, D., Chakraborty, S., Dash, S.K., Chattopadhyay, S., Chakraborty, M.: Butea monosperma bark extract mediated green synthesis of silver nanoparticles: characterization and biomedical applications. J. Saudi Chem. Soc. **21**(6), 673–684 (2017)

Piriyadharsini, R., Jeyakumar, S.J., Jothibas, M.: Investigating photocatalytic degradation performance of biosynthesized cobalt oxide nanoparticles with its physiochemical properties. Inorg. Chem. Commun. **154**, 110911 (2023)

Priya, R., Stanly, S., Dhanalekshmi, S.B., Mohammad, F., Al-Lohedan, H.A., Oh, W.C., Sagadevan, S.: Comparative studies of crystal violet dye removal between semiconductor nanoparticles and natural adsorbents. Optik **206**, 164281 (2020)

Rasheed, T., Bilal, M., Li, C., Nabeel, F., Khalid, M., Iqbal, H.M.: Catalytic potential of bio-synthesized silver nanoparticles using *Convolvulus arvensis* extract for the degradation of environmental pollutants. J. Photochem. Photobiol. B. **181**, 44–52 (2018)

Rather, M.Y., Sundarapandian, S.: Facile green synthesis of copper oxide nanoparticles and their rhodamine-b dye adsorption property. J. Cluster Sci. **33**(3), 925–933 (2022)

Ribeiro, A.R., Nunes, O.C., Pereira, M.F., Silva, A.M.: An overview on the advanced oxidation processes applied for the treatment of water pollutants defined in the recently launched directive 2013/39/EU. Environ. Int. **75**, 33–51 (2015)

Sabour, M.R., Amiri, A.: Comparative study of ANN and RSM for simultaneous optimization of multiple targets in Fenton treatment of landfill leachate. Waste Manage. **65**, 54–62 (2017)

Saeed, M., Akram, N., Naqvi, S.A.R., Usman, M., Abbas, M.A., Adeel, M., Nisar, A.: Green and eco-friendly synthesis of Co3O4 and Ag-Co3O4: characterization and photo-catalytic activity. Green Process. Synthes. **8**(1), 382–390 (2019)

Safdar, A., Mohamed, H.E.A., Hkiri, K., Muhaymin, A., Maaza, M.: Green synthesis of cobalt oxide nanoparticles using hyphaenethebaica fruit extract and their photocatalytic application. Appl. Sci. **13**(16), 9082 (2023)

Salavati-Niasari, M., Khansari, A., Davar, F.: Synthesis and characterization of cobalt oxide nanoparticles by thermal treatment process. InorganicaChimicaActa **362**(14), 4937–4942 (2009)

Samuel, M.S., Selvarajan, E., Mathimani, T., Santhanam, N., Phuong, T.N., Brindhadevi, K., Pugazhendhi, A.: Green synthesis of cobalt-oxide nanoparticle using jumbo *Muscadine* (*Vitis-rotundifolia*): characterization and photo-catalytic activity of acid Blue-74. J. Photochem. Photobiol. B. **211**, 112011 (2020)

Sarvalkar, P.D., Vadanagekar, A.S., Karvekar, O.S., Kumbhar, P.D., Terdale, S.S., Thounaojam, A.S., Sharma, K.K.K.: Thermodynamics of azo dye adsorption on a newly synthesized titania-doped silica aerogel by cogelation: a comparative investigation with silica aerogels and activated charcoal. ACS Omega **8**(14), 13285–13299 (2023)

Sarvalkar, P.D., Jamadar, A.S., Magdum, A.B., Pawar, P.K., Yadav, J.B., Nimbalkar, M.S., Sharma, K.K.K.: Biogenic synthesis of Co_3O_4 nanoparticles from aloe barbadensis extract: antioxidant and antimicrobial activities, and photocatalytic degradation of azo dyes. Result Eng. **22**, 102094 (2024)

Semwal, A., Kumar, A.: Identification of functional groups in butea monosperma methanolic leaf extract through fourier transform infrared spectroscopy (FT-IR). Pharma Innovat. J. **12**(5), 2104–2108 (2023)

Shahzadi, T., Zaib, M., Riaz, T., Shehzadi, S., Abbasi, M.A., Shahid, M.: Synthesis of eco-friendly cobalt nanoparticles using *Celosia argentea* plant extract and their efficacy studies as antioxidant, antibacterial, hemolytic and catalytical agent. Arab. J. Sci. Eng. **44**, 6435–6444 (2019)

Shanmuganathan, R., Sathiyavimal, S., Le, Q.H., Al-Ansari, M.M., Al-Humaid, L.A., Jhanani, G.K., Barathi, S.: Green synthesized cobalt oxide nanoparticles using Curcuma longa for anti-oxidant, antimicrobial, dye degradation and anti-cancer property. Environ. Res. **236**, 116747 (2023)

Sharma, M.V., Sharma, H.K.: Application of polypyrrole/lead sulphidenanocomposite in UV light assisted photocatalysis and gas sensing. J. Polym. Composites **9**, 13–27 (2021)

Sharma, M.V., Sharma, H.K., Jadon, N.: A study on degradation of methyl orange under UV light irradiation and ammonia gas sensing by polypyrrole/lead selenidenanocomposite. Adv. Bio. Res **12**, 1–12 (2021)

Sharma, R., Garg, R., Bali, M., Eddy, N.O.: Biogenic synthesis of iron oxide nanoparticles using leaf extract of *Spilanthesacmella*: antioxidation potential and adsorptive removal of heavy metal ions. Environ. Monit. Assess. **195**(11), 1345 (2023)

Singh, A., Kaur, M., Choudhary, A., Kumar, B.: Effect of *Butea-monosperma* leaf extracts on cyclophosphamide induced clastogenicity and oxidative stress in mice. Pharmacognosy Res. **7**(1), 85 (2015)

Sodhani, H., Hedaoo, S., Murugesan, G., Pai, S., Vinayagam, R., Varadavenkatesan, T., Selvaraj, R.: Adsorptive removal of Acid Blue 113 using hydroxyapatite nanoadsorbents synthesized using peltophorumpterocarpum pod extract. Chemosphere **29**, 134752 (2022)

Som, I., Biswas, S., Dey, S., Saha, R.: A mesoporous CuO/CuSe heterojunction nanocomposite with applications in visible-light photocatalysis and as an electrochemical phenol sensor. ChemistrySelect **8**(28), e202301253 (2023)

Soni, V., Xia, C., Cheng, C.K., Nguyen, V.H., Nguyen, D.L.T., Bajpai, A., Raizada, P.: Advances and recent trends in cobalt-based cocatalysts for solar-to-fuel conversion. Appl. Mater. Today **24**, 101074 (2021)

Srivind, J., Nagarethinam, V.S., Suganya, M., Balamurugan, S., Prabha, D., Balu, A.R.: Visible light irradiated photocatalytic performance of SnS2-CdO nanocomposite against the degradation of Rhodamine B (cationic) and Congo red (anionic) dyes. Mater. Sci. Eng. B **255**, 114530 (2020)

Sun, J.H., Dong, S.Y., Wang, Y.K., Sun, S.P.: Preparation and photocatalytic property of a novel dumbbell-shaped ZnO microcrystal photocatalyst. J. Hazard. Mater. **172**, 1520–1526 (2009). https://doi.org/10.1016/j.jhazmat.2009.08.022PMID:19735975

Tacchini, I., Terrado, E., Anson, A., Martínez, M.T.: Preparation of a TiO_2–MoS_2 nanoparticle-based composite by solvothermal method with enhanced photoactivity for the degradation of organic molecules in water under UV light. Micro Nano Lett. **6**(11), 932–936 (2011)

Tomar, R., Abdala, A.A., Chaudhary, R.G., Singh, N.B.: Photocatalytic degradation of dyes by nanomaterials. Mater. Today **29**, 967–973 (2020)

ul. Haq. Z, Qureashi. A, Nazir. I, Ganaie. F. A, Bashir. A, Malik. L. A, & Pandith. A. H, Fabrication of 2D graphene oxide incorporating S-scheme Sn 2 S 3–In 2 S 3 heterojunctions for enhanced photocatalytic mineralization of organic pollutants. New J. Chem. 48(13), 5988-5999 (2024)

Vinayagam, R., Pai, S., Murugesan, G., Varadavenkatesan, T., Kaviyarasu, K., Selvaraj, R.: Green synthesized hydroxyapatite nanoadsorbent for the adsorptive removal of AB113 dye for environmental applications. Environ. Res. **212**, 113274 (2022)

Vishwanathan, S., Laxmi, S., Nandan, S., Jayan, S., Lijo, M., Das, S.: Effect of experimental parameters on photocatalytic degradation efficiency of TiO_2 nanoparticles synthesized by electrochemical method towards Rhodamine B dye solution under natural sunlight. Environ. Sci. Pollut. Res. **30**(4), 8448–8463 (2023)

Viswanathan, B.: Photocatalytic degradation of dyes: an overview. Current Catalysis **7**(2), 99–121 (2018)

Wan, J., Xu, L.H., Pan, H., Wang, L.M., Shen, Y.: Green water-based fabrication of SiO_2–TiO_2 aerogels with superhydrophobic and photocatalytic properties and their application on cotton fabric. J. Porous Mater. **28**(5), 1501–1510 (2021)

Warang, T., Patel, N., Fernandes, R., Bazzanella, N., Miotello, A.: Co3O4 nanoparticles assembled coatings synthesized by different techniques for photo-degradation of methylene blue dye. Appl. Catal. B **132**, 204–211 (2013)

Yang, J., Wei, Q., Li, D., Yu, J., Cai, Z.: Study on adsorption performance of manganese titanium oxide composite biochar for removal of Rhodamine B. J. Indian Chem. Soc. **100**(4), 100958 (2023)

Publisher's Note Springer Nature remains neutral with regard to jurisdictional claims in published maps and institutional affiliations.